Interaction of Surface-Tension and Buoyancy Mechanisms in Horizontal Liquid Layers

G. S. R. Sarma*
Deutsche Forschungs- und Versuchsanstalt für Luft und Raumfahrt e.V.
Göttingen, Federal Republic of Germany

Horizontal liquid layers are prone to convective instability when subjected to appropriate vertical gradients of temperature and/or concentration. The two potentially destabilizing mechanisms leading to instability in the configuration, namely, surface tension and buoyancy, generally support each other, and their action can be tightly coupled. However, this finding, originally due to Nield, needs considerable qualification not only under the action of external forces such as Coriolis and Lorentz fields but also when the effects of wavy disturbances at the two-fluid interface are to be duly taken into account. Under different boundary conditions and in certain parameter ranges, significant departures from the coupling are demonstrated.

Nomenclature

B = magnetic induction field
B_0 = magnitude of B-field
K = thermal conductivity
c_0 = specific heat
d = mean thickness of the liquid layer
g = acceleration due to gravity
g_0 = terrestrial value of g
k_x, k_y = disturbance wave numbers in x,y (horizontal) directions
q = heat-transfer coefficient at the two-fluid interface
β = coefficient of thermal expansion
γ = electrical conductivity
ΔT = temperature difference $(T_0 - T_1)$
κ = thermal diffusivity $K/(\rho c_0)$
λ = disturbance wavelength $2\pi/\sqrt{(k_x^2 + k_y^2)}$
μ = dynamic viscosity
ν = kinematic viscosity
ρ = density
σ = interfacial energy at the two-fluid interface
Ω = angular speed of rotation

Dimensionless Parameters

a = $2\pi d/\lambda$ (disturbance wave number)
Bo = $\rho g d^2/\sigma$ (Bond)
Cr = $\kappa\mu/\sigma d$ (crispation/capillary)
Fl = $(W''' - 3a^2 W')/W'$ (flow indicator)
Ma = $d\,|\Delta T(d\sigma/dT)|/\kappa\mu$ (Marangoni)
Nu = qd/K (Nusselt/Biot)
Q = $B_0^2 d^2 \gamma/\mu$ (Chandrasekhar)
Ra = $g\beta\Delta T d^3/\nu\kappa$ (Rayleigh)
Ta = $2\Omega d^2/\nu$ (Taylor)

Introduction

CONFIGURATIONS of interest in materials processing often involve fluid interfaces and gradients of temperature and/or concentration, which in turn can induce interfacial tractions and also interact with any body forces present. These configurations are therefore inherently predisposed toward convective instabilities and macroscopic flows, which can lead to thermal fluctuations and concomitantly to often undesirable compositional changes in the end product.[1-3] Understanding the origins of such instabilities and investigation of possible methods of controlling them[2] both in the prototype configurations and in related model experiments in space and in ground-based research are of continuing interest. The interaction between surface-tension-driven and buoyancy-driven thermal and/or solutal instability in these systems is often unavoidable. For low-gravity simulation on Earth, reduction in model size has clearly a lower limit, even for qualitative studies. In experiments aboard orbital laboratories, large-size models are desirable for better diagnostics and data acquisition. In either case, therefore, there is likely to be a residual effective gravity interacting with the ubiquitous temperature/concentration gradients in these configurations. The nominal gravity level in the Spacelab[3] of ~ 0 $(10^{-4} g_0)$, for instance, can be offset by a tenfold increase in size if the characteristic length to the fourth power occurs in the dimensionless parameter describing the pertinent effect. Although the basic buoyancy/surface-tension interaction has been studied since the 1960s under special conditions, there still seem to be open questions in the area as shown by the early experiments aboard Apollo missions.[4]

In this general context, we consider the basic problem of thermal instability driven both by gravity and capillarity in a horizontal liquid layer under various boundary conditions. In view of the practical interest in controlling instability[2] in the configuration we include the effects of uniform rotation about a vertical axis and a uniform vertical magnetic field.[5]

Formulation of the Problem

We consider an infinite, horizontal, incompressible liquid layer of mean thickness d rotating about a vertical axis at a constant angular speed Ω. The lower and upper horizontal boundaries are nominally at constant temperatures T_0, T_1, respectively $(T_0 > T_1)$, while a uniform magnetic induction field of strength B_0 may also be applied transverse to the layer. The layer is bounded at least on one side by an ambient gas and is subjected to a variety of thermal and electromagnetic boundary conditions. We treat in the following three specific situations denoted by circled numbers 1, 2, and 3. Figure 1 is a schematic representation of the configuration and the boundary conditions (b.c.) considered.

The Boundary-Value Problems

The conditions for the onset of convection in this configuration can be formulated as a problem of stability[6] of the initial,

Received May 21, 1985; presented as Paper 85-0986 at the AIAA 20th Thermophysics Conference, Williamsburg, VA, June 19-21, 1985; revision received March 10, 1986.

*Research Scientist, Institute for Theoretical Fluid Mechanics. Member AIAA.

linear temperature profile across the layer. An earlier asymptotic investigation[7] indicates that the incipient instability in the configuration is likely to be in the stationary mode even if oscillatory modes are admitted by the system under some circumstances. Within the standard framework of the normal modes procedure,[6] the special features associated with the boundary conditions at a wavy two-fluid interface are of critical importance in the present case.[5,8,9] In contrast to earlier investigations, [10-13] we specifically allow for nonzero interfacial deflection, i.e., a *finite* surface tension σ in addition to a finite variation of σ with temperature in formulating the pertinent stress and thermal balance conditions. In dimensionless terms the aforesaid stability problem can be stated as follows with $DF \equiv F'$ denoting $d\cdot(\mathrm{d}F/\mathrm{d}z)$ for any $F(z)$:

$$(D^2-a^2)^2 W - Ta\cdot DZ - Q\cdot D^2 W = Ra\cdot a^2\theta \tag{1}$$

$$(D^2-a^2)\theta + W = 0 \tag{2}$$

$$(D^2-a^2)Z + Ta\cdot DW + Q\cdot DX = 0 \tag{3}$$

$$(D^2-a^2)X + DZ = 0 \tag{4}$$

For cases 1, 2, and 3, the boundary conditions (b.c.) are

$$W(1) = 0 = DZ(1) = X(1) \tag{5}$$

$$-Nu\cdot D^2 W(1) + Ma\cdot a^2 D\theta(1) = 0 \tag{6}$$

$$Nu\cdot Cr\cdot\{-D^3 W(1) + 3a^2 DW(1)\}$$
$$+ a^2(Bo+a^2)\{D\theta(1) + Nu\cdot\theta(1)\} = 0 \tag{7}$$

and for $Nu = 0$, Eqs. (6) and (7) are to be replaced by

$$D\theta(1) = 0 \tag{8}$$

$$(Bo+a^2)\{D^2 W(1) + Ma\cdot a^2\theta(1)\}$$
$$+ Ma\cdot Cr\cdot\{-D^3 W(1) + 3a^2 DW(1)\} = 0 \tag{9}$$

whereas at the lower boundary (individually different) for case 1,

$$W(0) = 0 = DW(0) = Z(0) = \theta(0) = DX(0) \tag{10}$$

for case 2,

$$W(0) = 0 = DW(0) = Z(0) = D\theta(0) = X(0) \tag{11}$$

and for case 3, the same conditions as Eqs. (5-9) hold at $z = 0$.

Here W, Z, X, and θ are, respectively, the dimensionless disturbance amplitudes of the z components of velocity, vorticity, and electric current density, and of temperature in the perturbed state. Equations (1-4) describe, respectively, the transport of momentum, energy, and current density in a stationary perturbed state of the basic configuration. The boundary conditions for cases 1, 2, and 3 are specifications of the thermal and electromagnetic characteristics of the adjoining media in each case. We consider the following cases. The ambient gas at $z = d$ in cases 1 and 2 and at $z = 0$, d in case 3 is an electrically perfect insulator. Moreover, at the interface the heat-transfer characteristics in the disturbed state are described by a heat-transfer coefficient q, which we also take to be the same for both the fluid interfaces for case 3 for the sake of simplicity.

In cases 1 and 2, the layer is bounded at $z = 0$ by a solid wall that is considered a thermally and electrically perfect conductor in case 1 and insulator in case 2. Application of these conditions on the velocity, vorticity, current density, and temperature yields[5,8,9] the boundary conditions in the form of Eqs. (10) and (11).

Boundary Conditions at the Fluid Interface

In contrast to earlier treatments with a flat two-fluid interface, the boundary conditions are applied here at a disturbed wavy interface. Since the location of the disturbed interface is unknown a priori, its amplitude ζ_0 (assumed to be small within the linear theory) is an additional dependent variable in the problem. The auxiliary condition for determining the same is provided by the kinematic condition; namely, the time rate of change of the interfacial elevation equals the velocity normal to the interface. For the neutrally stable, stationary mode (the time rate of change being zero), this condition reduces simply to $W(1) = 0$ in Eq. (5). The normal and tangential stress balance conditions at the two-fluid interface after Taylor expansion about the mean (undisturbed) interface[5,8,9] lead to the following relations between the dimensionless amplitudes W, θ, and ζ_0.

Normal stress balance:

$$Cr\cdot\{D^3 W(1) - 3a^2 DW(1)\} = a^2(Bo+a^2)\zeta_0 \tag{12}$$

Tangential stress balance:

$$a^2 Ma\cdot\{\theta(1) - \zeta_0\} + W''(1) + a^2 W(1) = 0 \tag{13}$$

$$Z'(1) = 0 \tag{14}$$

The thermal boundary condition at the wavy interface is somewhat simplified by assuming a nominal (constant) heat-transfer coefficient $q = \mathrm{d}S/\mathrm{d}T$, where S is the rate of heat loss per unit area at the two-fluid interface. The advantages and implications of this simplification were discussed in the pioneering work of Pearson,[13] and the same approach has been adopted ever since in all the later work. Pearson's assumption regarding the flat interface ($\zeta_0 = 0$) is relaxed here as per the refinements introduced originally by Scriven and Sternling.[8] Thus, we again get a relation between θ and ζ_0.

$$D\theta(1) + Nu\cdot\theta(1) = Nu\cdot\zeta_0 \tag{15}$$

The case $Nu = 0$ corresponds to the thermally "insulating" interface, whereas the limit $Nu \to \infty$ leads to the equality of temperature and interface amplitudes that holds trivially (since both θ and ζ_0 vanish for this "conducting" interface) in the buoyancy-driven case[6] and in Pearson's treatment.[13]

From the equations [(12), (13), and (15)] on eliminating the interface disturbance amplitude ζ_0, we get Eqs. (6) and (7) for $Nu \neq 0$ or Eqs. (8) and (9) for $Nu = 0$. Physical properties other than density $\rho(T)$ (within the Boussinesq approximation) and interfacial tension $\sigma(T)$ are taken as constants. The nondimensionalization is carried out using [6] the reference quantities d, $W_0 = \kappa/d$, $Z_0 = \kappa/d^2$, $\theta_0 = (T_0 - T_1)$, and $X_0 = \gamma B_0 \kappa/d$, respectively, for the length, velocity, vorticity, temperature, and current density. The choice of the thermal diffusive velocity W_0 is appropriate for the present configuration, in which the instability is thermally driven. Otherwise, the nondimensionalization plays no significant role here since the solutions of the full equations will be used in the following discussion.

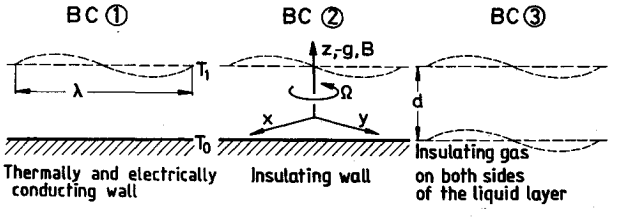

Fig. 1 Basic Bénard-Marangoni configuration under b.c. 1, 2, and 3.

The parameters *Ra, Ma, Ta, Q, Nu, Cr, Bo,* and *a* are appropriate ratios to measure, respectively, the effects of buoyancy, capillarity, rotation, magnetic field, heat transfer to the ambient fluid, interfacial curvature, interfacial gravity waves, and the single characteristic of a neutral, stationary, normal mode of the disturbance. Oscillatory modes[7] were also considered in special cases, but here we restrict our attention to the stationary mode. The homogeneous boundary-value problems (1-11) admit nontrivial solutions only when the above-mentioned parameters satisfy a secular condition of the form:

$$f(Ma,Ra,Q,Ta,Bo,Cr,Nu,a)=0 \qquad (16)$$

Results and Discussion

The secular conditions of the aforementioned form for the existence of nontrivial solutions for the respective homogeneous boundary-value problems have been obtained by using the general solutions of the governing equations in the appropriate boundary conditions in each of cases 1, 2, and 3. The details of the solution procedure for the general case and for the asymptotic long-wave limits are given elsewhere.[5] The general solutions W, θ, Z, and X for Eqs. (1-4) are linear combinations of exponential functions that can be expressed in terms of trigonometric and hyperbolic functions. The ten arbitrary constants of integration involved are to be determined from the linear system of homogeneous equations resulting from the appropriate boundary conditions (5-11). Nontrivial solutions for this system exist if and only if the pertinent coefficient determinant vanishes. This requirement leads to the secular condition (16), which is to be satisfied by the parameters of the problem. We determine *Ma* (regarded as the eigenvalue parameter) as a function of the disturbance wave number *a* in order to obtain the linear stability characteristics of the basic configuration defined by given values of *Ra, Ta, Q, Bo, Cr,* and *Nu*. Special interest centers around the minimum of $Ma-Ma_c$ defining the threshold for the onset of convective instability in the layer.

Parameter Values

In view of the large number of parameters involved, we must restrict our attention to some special situations with representative orders of magnitude for the above parameters. Results for some of the special cases have been reported earlier[5,7] and discussed in the light of other results in the literature. In illustrating the significance of the interfacial curvature ($Cr\neq 0$) and of gravity waves ($Bo\neq 0$) in contrast to the cases $Cr=0$, $Bo=0$, the small values of $Cr=10^{-3}$, 10^{-4}; $Bo=0.05$, 0.01[8,9] have been found particularity instructive. For the chosen values of *Cr*, the corresponding *Bo* values can be estimated for different classes of substances and various *g* levels since it turns out that the dimensionless ratio $Bo/Cr=gd^3/\kappa\nu=Ra/(\beta\Delta T)$ is the key parameter determining the long-wave stability characteristics of the system. The values chosen for $Bo=0.01$, 0.05 with $Cr=10^{-3},10^{-4}$ may also be regarded as representative estimates for experiments in an Earth laboratory on thin liquid layers ($d\sim$mm) and experiments in an orbital laboratory with thicker layers ($d\sim$cm, $g\sim 10^{-4}g_0$, the nominal gravity level quoted for Spacelab[3]), using thermophysical data on silicone oils[14] and some semiconductor and metallic melts[15,16] for reference. Table 1 gives representative estimates of *Bo/Cr,Q*, and *Ta*. It may be mentioned that results appropriate to other situations can be computed readily by the same procedure as the one used here and then be applied in the appropriate parameter domains.

Neutral Stability Characteristics

The dependence of the stability characteristics on *Nu, Ta,* and *Q* has been discussed in detail elsewhere,[5] with special reference to small *Ra* demonstrating the importance of the long-wave modes ($a\to 0$) for the present configuration. Asymptotic analysis shows that $Ma\propto a^2$, $a\to 0$ for $Bo=0$, $Cr\neq 0$, whereas $Ma\to Ma_1\neq 0$ when $Bo\neq 0$ and $Cr\neq 0$. Figures 2 and 3 show some typical neutral stability curves for the three boundary conditions 1, 2, and 3. Boundary condition 2 is qualitatively between 1 and 3, sharing some of the features of 1 and 3 in different parameter ranges. The domain above each curve corresponds to instability and that below to stable states in the linear sense, i.e., against small inherent disturbances. It is found[5] that the stable domain increases with *Nu*. This is due to the stabilizing effect of heat transfer across the two-fluid interface to the ambient gas. Thus, the least stable situation prevails at $Nu=0$. We restrict ourselves to this case in the following.

The Flat and Curved Interface

Figures 2 and 3 show that the flat interface curves ($Cr=0$) differ drastically from those of the wavy interface ($Bo\neq 0$,

Table 1 Representative magnitudes of *Bo/Cr, Ta,* and *Q* ($g=9.81$ m/s^2, $d=1$ mm, $B_0=0.1$ *T*, $\Omega=50$ rpm)

	Al melt	Cu melt	Ge melt	Si melt	Ga As melt	DC 200, 25°C
Bo/Cr	242	607	8740	1821	710	450
Ta	19.5	24.8	78.2	29.8	33.7	0.052
Q	36.1	14.0	22.3	13.6	5.7	—

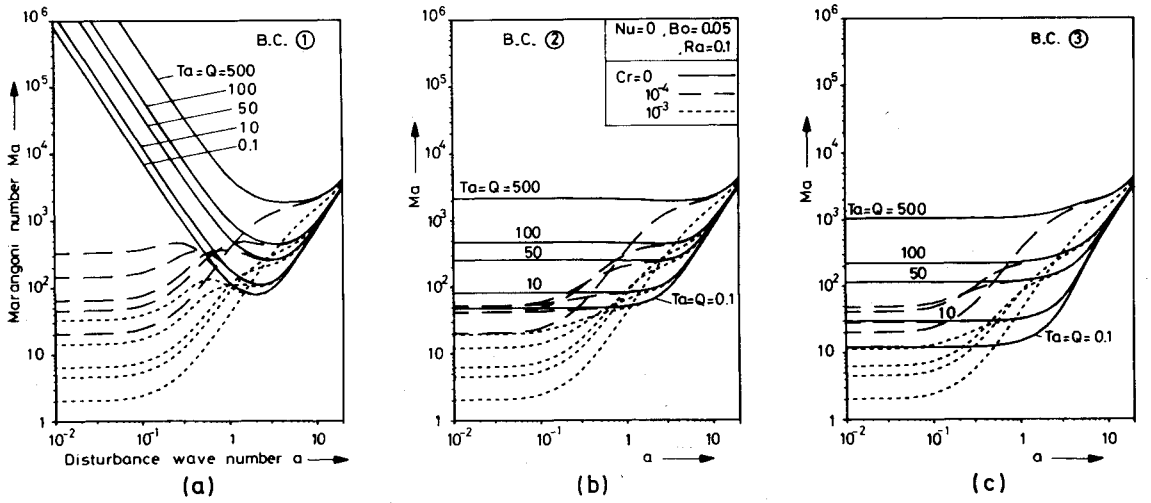

Fig. 2 Neutral curves for thermocapillary convective instability in a horizontal liquid layer under b.c. 1, 2, and 3 ($Nu=0$, $Ra=0.1$, $Bo=0.05$).

$Cr \neq 0$). The latter show the possibility of *two local minima* in Ma (e.g., for b.c. 1, $Cr = 10^{-4}$, $Ta = Q = 0.1$, at $a \to 0$ and $a \simeq 2$). The important observation for later discussion is that, in contrast to the case $Bo = 0$, $Cr \neq 0$,[7,8] there *does* exist a nonzero critical Marangoni number $Ma = Ma_c$ when *both* Bo and Cr[5,9] are nonzero. This Ma_c is given by the absolute minimum in Ma along the respective neutral stability curves for given Ta, Q, Cr, Nu, Bo, and Ra. The corresponding critical wave number a_c may tend to zero in certain parameter ranges (cf. Fig. 2a, b.c. 1 at large Ta, Q, and Figs. 2b, c, and 3a). Thus, at nonzero gravity the convective instability sets in only above a finite threshold value Ma_c, even with a wavy two-fluid interface with critical wavelengths λ_c being finite or infinite depending on the parameter ranges and the boundary conditions.

In Fig. 2 we also notice the stabilizing tendency of the Coriolis and Lorentz forces in that Ma_c increases with Ta and Q in general. However, a monotonic increase in Ma_c is limited to a certain range of Ta and Q when the fluid interface is wavy (cf. b.c. 2 and 3; $Cr = 10^{-3}$, 10^{-4}; $Ta = Q = 50$ vs 100), and Ma_c may decrease with Ta and Q. Thus, the anticipated stabilizing action of these agencies has also to be optimized within an appropriate parameter range, especially for thin liquid layers. Figure 3 illustrates the effect of variation of Ra, i.e., of buoyancy, on the neutral curves with b. c. 2 as a case intermediate between b.c. 1 and 3. We observe that Ma_c at $Ra = 150$ can be *higher* than that at $Ra = 50$ or at $Ra = 0.1$ (Fig. 2b) for $Cr \neq 0$. Furthermore, the stable domain at $Cr \neq 0$ can be larger than at $Cr = 0$ (cf. Figs. 3b and 3c). Also the critical wavelength λ_c can become finite even under b.c. 2 as Ra increases above a threshold and buoyancy takes hold (cf. Figs. 3b and 3c, $Cr = 10^{-3}$). The full range of variation of a_c with Rayleigh number under b.c. 2 is illustrated in Fig. 4, where Ra^* is the normalized Ra defined in the next subsection. Since Ma_c can occur at $a_c = 0$ in certain cases, an asymptotic analysis was carried out[5] by perturbing the eigenvalue problems (1-11) in the limit $a \to 0$. Thus we get the following limits Ma_1 along the respective neutral stability curves for $Nu = 0$, $Ta = 0 = Q$, $Ra \sim 0(1)$:

$$\text{b.c. 1: } Ma_1 = f_1(Bo/Cr) \tag{17}$$

where $f_1(Bo/Cr) = (2/3)Bo/Cr$,

$$\text{b.c. 2: } Ma_1 = (960 - 3Ra)/f_2(Ra, Bo/Cr) \tag{18}$$

where $f_2(Ra, Bo/Cr) = [20 + (1440 - 12Ra)Cr/Bo]$,

$$\text{b.c. 3: } Ma_1 = 12(1 - Ra/120)/f_3(Ra, Bo/Cr) \tag{19}$$

where $f_3(Ra, Bo/Cr) = [1 - Ra\, Ma_1 (Cr/Bo)^2]$.

The above results show the role of the ratio Bo/Cr in determining the long-wave stability characteristics of the configuration when both Bo and Cr are nonzero. We note that this ratio is independent not only of ΔT but also of σ, and hence its influence is not limited by the size of σ. As $Bo/Cr \to 0$, $Ma_1 \to 0$ and at *zero gravity* there is strictly *no critical Ma* below which the liquid layer is stable against arbitrary long-wave disturbances. In general, at smaller Bo/Cr, the long-wave modes become more important. Numerical results in Figs. 2 and 3a agree well with the asymptotic results in the limit $a \to 0$.

The Bénard-Marangoni Interaction

Based on the general information gathered from the neutral stability curves such as Figs. 2 and 3, we now discuss in the following only the variation of the *critical Marangoni number* Ma_c with respect to Ra under different boundary conditions in order to study the coupling between the two potentially destabilizing agencies due to thermocapillarity and buoyancy. For this purpose we normalize Ma_c, ($Ra \neq 0$), and Ra, respectively, in terms of Ma_0 (Ma_c at $Ra = 0$), and Ra_0 (Ra_c at $Ma = 0$) and set $Ra/Ra_0 = Ra^*$ and $Ma_c/Ma_0 = Ma^*$. The values of Ra_0 and Ma_0 are listed in Tables 2 and 3 for the different b.c. and parameters. (We may mention that Ra_0 and Ma_0 computed at $Ta = 0.1 = Q$ from our general solutions for Ta, $Q \neq 0$ are slightly higher than those for zero Ta and Q. Under b.c. 1, 2, and 3 at $Ta = Q = 0$, Ra_0 equals 669, 320, and 120, respectively.[5] The corresponding values of Ma_0 for $Cr = 0$ are 79.6, 48, and 12. The respective values for b.c. 2 and 3 can

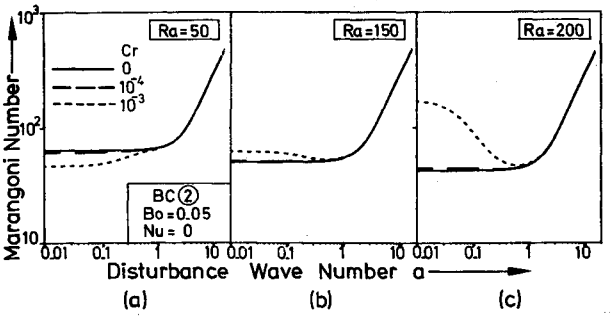

Fig. 3 Neutral curves for thermocapillary convective instability in a horizontal liquid layer under b.c. 2 ($Bo = 0.05$; $Nu = 0$; $Ta = 0.1 = Q$).

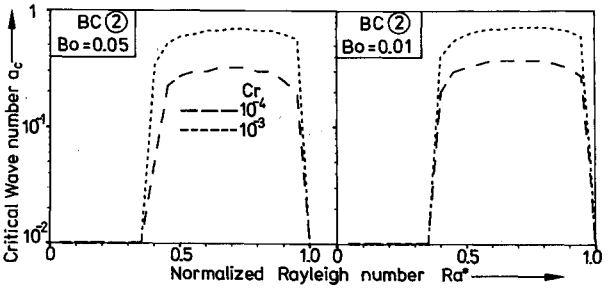

Fig. 4 Variation of critical wavenumber a_c with normalized Rayleigh number Ra^* for a horizontal liquid layer under b.c. 2 ($Bo = 0.05$, 0.01; $Nu = 0$; $Ta = 0.1 = Q$).

Table 2 Values of Ma_0 and Ra_0 under b.c. 1, 2, and 3 ($Nu = 0$, $Ta = 0.1 = Q$)

	$Ma_0/(a_c)$ under b.c. 1			$Ma_0/(a_c)$ under b.c. 2			$Ma_0/(a_c)$ under b.c. 3		
Bo	$Cr = 0$	10^{-4}	10^{-3}	$Cr = 0$	10^{-4}	10^{-3}	$Cr = 0$	10^{-4}	10^{-3}
0.01	79.9	66.3	6.63	48.23	27.93	5.83	12.1	12.1	10.83
	(2.0)	(0.0)	(0.0)	(0.0)	(0.0)	(0.0)	(0.0)	(0.0)	(0.0)
0.05	79.9	79.74	32.91	48.23	42.07	19.57	12.11	12.11	12.05
	(2.0)	(2.0)	(0.0)	(0.0)	(0.0)	(0.0)	(0.0)	(0.0)	(0.0)
	$Ra_0 = 671.2$, $a_c = 2.02$			$Ra_0 = 321.6$, $a_c = 0.0$			$Ra_0 = 121.7$, $a_c = 0.0$		

Table 3 Values of Ma_0 and Ra_0 under b.c. 1 at different Ta, Q ($Nu=0$, $Bo=0.05$)

$Ma_0/(a_c)$ at $Ta=50=Q$			$Ma_0/(a_c)$ at $Ta=100=Q$			$Ma_0/(a_c)$ at $Ta=500=Q$		
$Cr=0$	10^{-4}	10^{-3}	$Cr=0$	10^{-4}	10^{-3}	$Cr=0$	10^{-4}	10^{-3}
266.8	64.5	6.45	460.2	45.6	4.56	1955.7	20.39	2.04
(2.95)	(0.0)	(0.0)	(3.4)	(0.0)	(0.0)	(4.2)	(0.0)	(0.0)
$Ra_0=2371$, $a_c=3.20$			$Ra_0=4361$, $a_c=3.45$			$Ra_0=21861$, $a_c=3.025$		

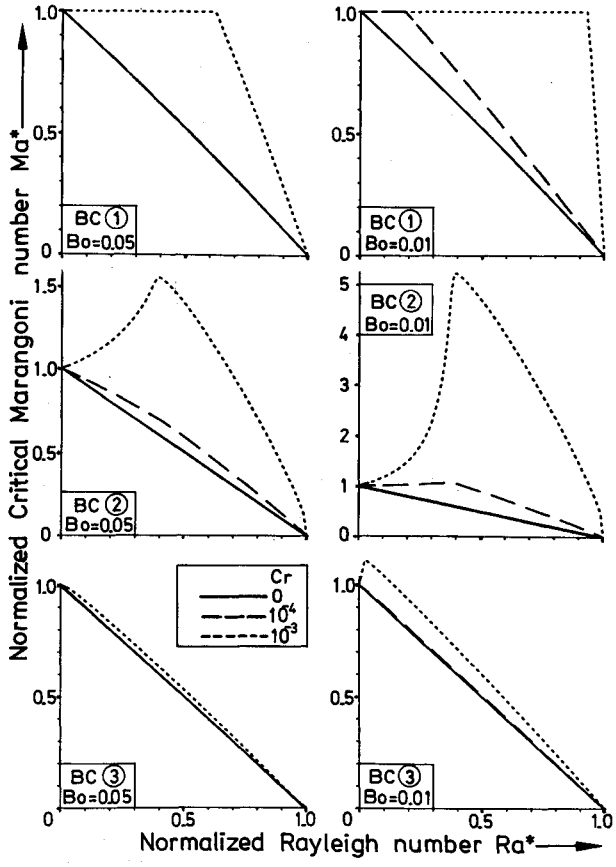

Fig. 5 Variation of Ma^* with Ra^* under b.c. 1, 2, and 3 ($Bo=0.05$, 0.01; $Nu=0$; $Ta=0.1=Q$).

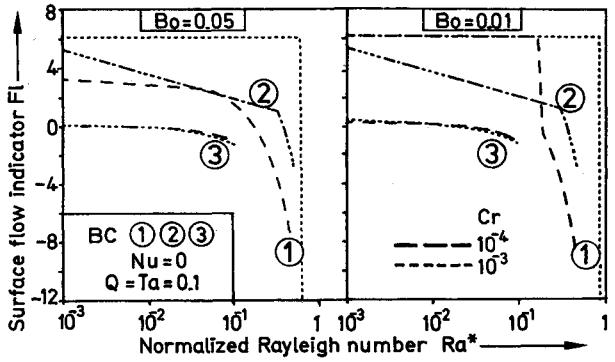

Fig. 6 Variation of interface flow indicator Fl with Ra^* under b.c. 1, 2, and 3 ($Bo=0.05$, 0.01; $Nu=0$; $Ta=0.1=Q$).

also be verified from Eqs. (18) and (19) since $a_c \to 0$ for these cases). Figure 5 illustrates the correlation between Ma^* and Ra^* at $Ta=0.1=Q$, i.e., the onset of the pure Bénard-Marangoni convective instability (under negligible Coriolis and Lorentz fields), when the effects of gravity waves ($Bo \neq 0$) and of finite interfacial tension ($Cr \neq 0$) at the two-fluid interface are taken into account. We notice that under b.c. 1, 2, and 3, a linear correlation, i.e., a "tight coupling" in the sense of mutual support between the two detstabilizing agencies,[10] obtains only for the flat interface (continuous curves with $Cr=0$). At $Cr \leq 10^{-4}$, the above correlation holds approximately for $Bo=0.05$ under b.c. 1 and 3 but not for $Bo=0.01$.

The drastic departure from the strictly monotonic correlation between Ra^* and Ma^* is to be clearly seen under b.c. 2 at $Cr=10^{-3}$ for Ra^* less than some threshold value ($\simeq 0.39$), wherein we find that Ma^* in fact *increases* with Ra^*. Ma^* stays well above unity for $Cr=10^{-3}$ over a considerable range of Ra^* before decreasing ultimately to zero as $Ra^* \to 1$. (In the "downhill" part, a_c is in fact nonzero.) Similar behavior is also to be seen for b.c. 3 at $Bo=0.01$. Under b.c. 2 and 3, therefore, there can be a regime in which an increase in buoyancy up to a certain threshold Ra_t can indeed *delay* the onset of convective instability beyond the critical gradients required at zero gravity. The threshold Ra_t is higher for lower Bo/Cr. Although too small to be seen on the plot for b.c. 1, there exists a similar regime near $Ra^* \to 0$. But the more obvious finding in the case of b.c. 1 is that buoyancy need not *reduce* the critical Marangoni number until Ra exceeds a certain threshold value. At the other extreme as $Ra^* \to 1$, i.e., when buoyancy dominates, our numerical results agree with the predictions of the asymptotic analysis[17] for b.c. 1 in the limit of small Cr, which indicates a possible *stabilizing* tendency of the interfacial curvature. This is even more pronounced under b.c. 2 at larger Ra^*(cf. Figs. 3b and 3c, $Cr=0$ vs $Cr=10^{-3}$, 10^{-4}). Thus, the present results spanning the entire range $0 \leq Ma^*, Ra^* \leq 1$ clearly indicate the dual role of the wavy interface. Whereas the layer tends to be destabilized by $Cr \neq 0$ in the long-wave limit, it is restabilized by $Bo \neq 0$ ($Ra \neq 0$). The quantitative significance of nonzero Bo and Cr is far greater in the low-buoyancy limit, say, in a low-gravity environment (real or simulated) and in thin liquid layers.

This ambivalence in the buoyancy/capillarity interaction may be partly a plausible explanation for the quicker onset of convection in the Apollo demonstration experiments.[4] Whereas in the ground experiment, onset of convection in the *same thin layer* could have been delayed somewhat by the counteracting buoyancy effect, there could be no such benefit from buoyancy at $g \sim 10^{-8} g_0$ aboard Apollo. At very small $Bo/Cr = gd^3/\kappa\nu$, as the asymptotic results show, Ma_c is also small. Thus, for given layer thickness, quicker onset of convection than on the ground is indeed likely at such low gravity levels. Sidewalls and practical lower bounds on observing incipient convection could lead to higher Ma_c and finite cell size. Since both the ground and space experiments were also presumably well in the supercritical regime, quantitative theoretical comparisons do not seem tenable here. But physically, even in that regime, it is likely that the evolution of the finite cells observed took longer in the ground experiment than in space due to the counteraction contribution of buoyancy in the former. Futhermore,[4] the undercurrents associated with the sidewall effects, nonuniform layer depth in space, together with some heat transfer to the environment ($Nu \neq 0$), might also have changed the pertinent a_c and Ma_c to begin with. Some experimental observations on superposed layers[18] under temperature gradients and on layers subjected

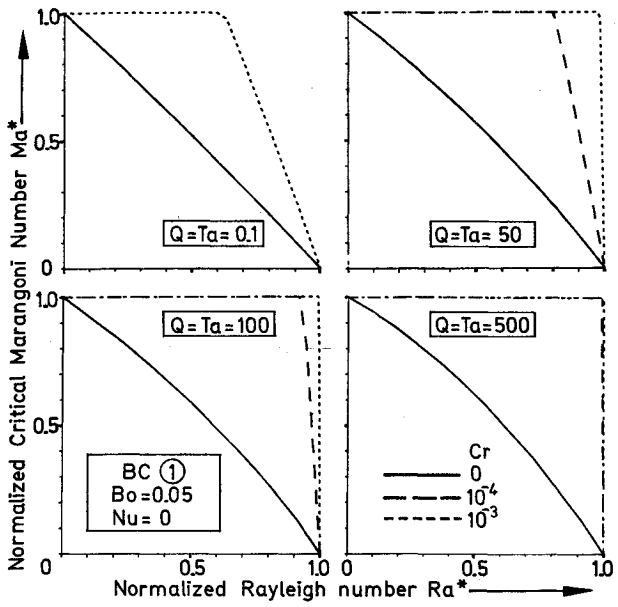

Fig. 7 Variation of Ma^* with Ra^* under b.c. 1 at different Ta, Q ($Bo=0.05$; $Nu=0$).

to concentration gradients[19] also suggest the possibility of counteraction between the destabilizing agencies.

The Counteraction Mechanism

The possible counteraction between the two inherently detstabilizing agencies of capillarity and buoyancy can be associated with the opposite flows[8] induced in the immediate vicinity of the two-fluid interface, where the thermocapillary tractions operate. In view of the kinematic condition for a stationary, neutral mode, $W(1)$ vanishes at the fluid interface. Therefore, the fluid immediately below moves toward the interface if $W'(1)$ is negative and away from it if $W'(1)$ is positive. Consequently, the flow is upward below the troughs of an interfacial wave and downward below the crests if ζ_0 and $W'(1)$ are of the same sign. In Fig. 6 we show the values of the surface flow indicator Fl [cf. Eq. (12)] given by

$$Fl=[W'''(1)-3a^2W'(1)]/W'(1) \tag{20}$$

under the three boundary conditions. We find that Fl is positive as $Ra^*\to 0$ and goes through zero to negative values as Ra^* exceeds a certain finite threshold value. The trend is clearly visible for b.c. 1 and 2 but is present numerically in case 3 as well. The Fl-sign reversal point in cases 2 and 3 is close to the changeover of λ_c to finite values. But the results for b.c. 1, wherein $a_c\simeq 2.0$ even for $Cr=10^{-4}$, $Bo=0.05$ as $Ra^*\to 0$ while Fl changes sign at $Ra^*\simeq 0.2$ also with $a_c\simeq 2.0$, show that the dominant regime of the respective driving mechanism, capillarity or buoyancy, is to be identified with the flow reversal rather than the wavelength. Besides, as already pointed out, λ_c can be finite even under b.c. 2 and 3 with some heat transfer to the ambient gas. Hence, the sign reversal of Fl is rightfully to be attributed to the increasing influence of buoyancy over that of surface tension.

Decoupling Due to Imposed Fields

In Fig. 7 the pronounced influence of the interfacial effects in decoupling the two destabilizing agencies even under b.c. 1 are illustrated for different Ta and Q. It is known[10-12] that under the action of Coriolis (Ta) and Lorentz (Q) fields, the said coupling weakens. This tendency is confirmed by the curves for $Cr=0$ (the flat interface) as Ta and Q increase. But we find that for given Ta and Q, the departures for nonzero Bo and Cr from the case $Cr=0$, $Ta=0.1=Q$ are far greater. As indicated in Fig. 5 calculations for other representative Bo values show that a greater decoupling effect (cf. higher rise in Ma^* for $Bo=0.01$) is associated with lower values of Bo/Cr as may be expected from the asymptotic results in Eqs. (17-19) if the pertinent $a_c\to 0$.

Conclusions

Convective instability due to vertical density and interfacial energy gradients in a thin horizontal liquid layer bounded at least on the upper side by an ambient gas tends to occur at wavelengths that are large compared to the mean layer thickness under certain boundary conditions and in various parameter ranges. The parameter ratio Bo/Cr is of decisive importance for the onset of long-wave instability. At low values of Bo/Cr, quicker onset of convective instability in thin liquid layers is to be expected unless appropriate countermeasures are taken. Such layers[5] can, however, be stabilized in suitable parameter ranges by means of vertical magnetic fields and rotation about a vertical axis. Critical wavelength at onset can be finite or infinite, depending on the boundary conditions as well as the parameter ranges. Under some conditions, low to moderate buoyancy effects may tend to *raise* the critical vertical temperature gradient necessary to induce convective instability in thin liquid layers. The two destabilizing mechanisms inherent in such thin layers do not necessarily support each other and may even oppose each other under certain conditions. Physically this stems from the fact that the associated long-wave instabilities can induce potentially opposing types of flow under the two mechanisms. Our findings offer at least a partial explanation for the "unexpected" trend in the results of the early space experiments,[4] admittedly influenced by several nonideal conditions left out in theoretical analysis. Our theoretical results here point out the special relevance of the interfacial waviness and of imperfect boundary conditions in this context. Further investigations in the area should be of considerable interest for materials science experiments and materials processing in space. Demonstration experiments under precisely controlled conditions for studying the interaction between the basic mechanisms and viable means of suppressing instability in relevant configurations would also be highly valuable.

Acknowledgments

This report received partial support through a collaborative Research Grant 419/84 from the NATO-Scientific Affairs Division, Brussels, Belgium. The author expresses his sincere thanks to the project coordinator, Professor R. Narayanan, University of Florida, Gainesville, Florida.

References

[1]Carruthers, J. R., "Origins of Convective Temperature Oscillations in Crystal Growth Melts," *Journal of Crystal Growth*, Vol. 32, No. 1, 1976, pp. 13-26.

[2]Jakeman, E. and Hurle, D. T. J., "Thermal Oscillations and their Effect on Solidification Processes," *Review of Physics in Technology*, Vol. 3, No. 3, 1972, pp. 3-30.

[3]Ostrach, S., "Low-Gravity Fluid Flows," *Annual Reviews of Fluid Mechanics*, Vol. 14, Annual Reviews Inc., Palo Alto, CA, 1982, pp. 313-345.

[4]Grodzka, P. G. and Bannister, T. C., "Heat Flow and Convection Experiments aboard Apollo 17," *Science*, Vol. 187, Jan. 1975, pp. 165-167.

[5]Sarma, G. S. R., "Effects of Interfacial Curvature and Gravity Waves on the Onset of Thermocapillary Convective Instability in a Rotating Liquid Layer Subjected to a Transverse Magnetic Field," *Physico Chemical Hydrodynamics*, Vol. 6, No. 3, 1985, pp. 283-300.

[6]Chandrasekhar, S., *Hydrodynamic and Hydromagnetic Stability*, Oxford University Press, London, 1961, Chaps. I-V.

[7]Sarma, G. S. R., "On Oscillatory Modes of Thermocapillary Instability in a Liquid Layer Rotating about a Transverse Axis," *Physico Chemical Hydrodynamics*, Vol. 2, No. 2/3, 1981, pp. 143-151.

[8]Scriven, L. E. and Sternling, C. V., "On Cellular Convection Driven by Surface-Tension Gradients: Effects of Mean Surface Tension and Surface Viscosity," *Journal of Fluid Mechanics*, Vol. 19, Pt. 3, 1964, pp. 321-340.

[9]Smith, K. A., "On Convective Instability Induced by Surface-Tension Gradients," *Journal of Fluid Mechanics*, Vol. 24, Pt. 2, 1966, pp. 401-414.

[10]Nield, D. A., "Surface Tension and Buoyancy Effects in Cellular Convection," *Journal of Fluid Mechanics*, Vol. 19, Pt. 3, 1964, pp. 341-352.

[11]Nield, D. A., "Surface Tension and Buoyancy Effects in the Cellular Convection of an Electrically Conducting Liquid in a Magnetic Field," *Zeitschrift für Angewandte Mathematik und Physik*, Vol. 17, No. 1, 1966, pp. 131-139.

[12]Namikawa, T., Takashima, M., and Matsushita, S., "The Effect of Rotation on Convective Instability Induced by Surface Tension and Buoyancy," *Journal of the Physical Society of Japan*, Vol. 28, May 1970, pp. 1340-1349.

[13]Pearson, J. R. A., "On Convection Cells Induced by Surface Tension," *Journal of Fluid Mechanics*, Vol. 4, Pt. 5, 1958, pp. 489-500.

[14]Palmer, H. J. and Berg, J. C., "Convective Instability in Liquid Pools Heated from Below," *Journal of Fluid Mechanics*, Vol. 47, Pt. 4, 1971, pp. 779-787.

[15]Cutler, M., *Liquid Semiconductors*, Academic Press, New York, 1977, Chap. 2.

[16]Chang, C. E. and Wilcox, W. R., "Inhomogeneities due to Thermocapillary Flow in Floating Zone Melting," *Journal of Crystal Growth*, Vol. 28, No. 1, 1975, pp. 8-12.

[17]Davis, S. H. and Homsy, G. M., "Energy Stability Theory for Free-Surface Problems: Buoyancy Thermocapillary Layers," *Journal of Fluid Mechanics*, Vol. 98, Pt. 3, 1980, pp. 527-553.

[18]Zeren, R. W. and Reynolds, W. C., "Thermal Instabilities in Two-Fluid Horizontal Layers," *Journal of Fluid Mechanics*, Vol. 53, Pt. 2, 1972, pp. 305-327.

[19]Davenport, I. F. and King, C. J., "Marangoni Stabilization of Density-Driven Convection," *Chemical Engineering Science*, Vol. 28, Feb. 1973, pp. 645-647.